Nuclear Instruments and Methods in Physics Research B 356–357 (2015) 114–128

Contents lists available at ScienceDirect

Nuclear Instruments and Methods in Physics Research B

journal homepage: www.elsevier.com/locate/nimb

Elaboration and behavior under extreme irradiation conditions of nano- and micro-structured TiC

S. Gavarini [a,c,*], N. Millard-Pinard [a], V. Garnier [b], M. Gherrab [a,b], J. Baillet [a], L. Dernoncourt [a], C. Peaucelle [a], X. Jaurand [c], T. Douillard [b]

[a] Université de Lyon, Université Claude Bernard Lyon 1, CNRS/IN2P3, UMR5822, IPNL, F-69622 Lyon, France
[b] INSA de Lyon, MATEIS CNRS UMR5510, 7 Avenue Jean Capelle, F-69621 Villeurbanne, France
[c] Université de Lyon, Université Lyon 1, Centre Technologique des Microstructures (CTμ), 5 rue Raphael Dubois, 69622 Villeurbanne Cedex, France

ARTICLE INFO

Article history:
Received 17 February 2014
Received in revised form 2 March 2015
Accepted 24 April 2015
Available online 14 May 2015

Keywords:
Ceramic
Carbide
Irradiation
Noble gas
Grain size

ABSTRACT

Titanium carbide samples were prepared by spark plasma sintering. Three different microstructures were prepared with average grain sizes of about 0.3, 1.3 and 25.0 µm. Each microstructure was irradiated with either 500 keV $^{40}Ar^{+}$ ions or 800 keV $^{129}Xe^{++}$ ions. The irradiation fluence varied from 6×10^{16} to 3.2×10^{17} at.cm^{-2}. Irradiation was carried out at room temperature (RT) or at 1000 °C. Post-irradiation annealing was performed on some samples to follow the surface modification. In fact, clusters and nanocracks were observed at depth in the nanometric grains (<100 nm) whereas more extended cracks were found in larger grains (>1 µm). Microcracks can induce localized surface blistering after irradiation at RT and for the highest fluencies. The size, shape and density of the blisters were proposed to depend on the crystallographic orientation of each grain. The microstructure with sub-micrometric grains exhibited increased surface roughness after irradiation, with grain removal and grain boundary abrasion but no blistering. Surface blistering is not observed after irradiation at 1000 °C but the complete delamination of extended areas containing large grains occurs. In this article, we highlight the role played by gastight grain boundaries and porosity to explain the distinct behavior of microstructures.

1. Introduction

Due to their thermophysical and nuclear properties, refractory ceramics are attractive materials for applications in future nuclear power reactors (fusion [1–3] or fission concepts [3,4]) [5]. Since the Fukushima accident, ceramic cladding has been the subject of substantial research as it could offer improved safety and performance as well as addressing the current problems with zirconium alloy cladding in light water reactors (LWRs) [6–11]. For example, under severe accident scenarios in LWRs, the increase in temperature causes oxidation of the Zr alloy cladding (inside by UO_2 but primarily outside by steam [11]) and results in rapid production of hydrogen. However, highly refractory ceramic clad fuel could survive much higher temperatures.

As an illustration of the possible high performance of ceramic cladding, silicon carbide (SiC) fiber-reinforced SiC-matrix composites (SiC/SiC composites) were obtained by Japanese researchers using a Nano-powder Infiltration and Transient Eutectoid (NITE) process that enabled production of an almost fully-dense SiC matrix [12]. Using this technology, SiC/SiC composites exhibit acceptable strength at room temperature (RT), pseudo-ductile fracture mode and extremely low gas permeability. Another technology called SiC *Triplex* nuclear fuel was developed recently in the USA to obtain cladding with three distinct layers [13]. This SiC *Triplex* design allows independent optimization of 3 properties: the inner monolith for fission gas retention, the fiber-reinforced matrix for overall mechanical performance, and the outer monolith for corrosion resistance. In France, ceramics are being studied for years as cladding in some fission reactors of Generation IV such as high temperature reactor (HTR) or gas cooled fast reactor (GFR) [14–16]. Recently, SiC_f/SiC has also been proposed for hexagonal wrapper in sodium cooled fast reactor (SFR) [17]. A multi-layer design, called *Sandwich* structure, was proposed with an inner metallic liner and SiC/SiC layers (French atomic agency "CEA" Patent [14]) allowing a gastight material even when the SiC matrix is cracked.

One of the possible issues of using SiC in cladding could be the relative decrease of its thermal conductivity at high temperature, under irradiation and also because of SiC matrix cracking in

* Corresponding author at: Université de Lyon, Université Claude Bernard Lyon 1, CNRS/IN2P3, UMR5822, IPNL, F-69622 Lyon, France.

http://dx.doi.org/10.1016/j.nimb.2015.04.064
0168-583X/

SiC/SiC composites [18–20]. Other highly refractory carbide [21] and nitride [22,23] ceramics have been studied over the past few years as possible alternatives to SiC, either in the form of thin coatings (diffusion barriers [24]) or as possible matrices in fiber-reinforced composites [18]. Titanium carbide (TiC) is among the candidate materials because of its typical ceramic properties (very high melting point and hardness [5]), but also because of its good thermal conductivity. Experiments carried out in France on the GANIL (Large National Heavy Ion Accelerator) facility at 500 °C showed that the thermal conductivity of TiC was higher than that of SiC [18,19]. Promising results were also obtained concerning TiC resistance to irradiation with krypton ions at RT [25,26]. In fact, a slight variation of thermal conductivity was observed but the surface topography remained unchanged after irradiation. TiC was not susceptible to amorphization during He ion irradiation over a wide temperature range 12–1523 K [27]. Upon annealing, several defect recovery stages were identified, and the specific diffusion processes responsible for the recovery were speculated as the diffusion of interstitial clusters. Other high temperature recovery and annealing experiments on TiC have indicated the possibility of activation of C vacancy migration at ≈600 °C and Ti vacancy migration above 1000 °C [21,28,29].

Table 1
Densification ratio and average grain size for each of the three microstructures.

Microstructure	SPS cycle	Densification ratios	Average grain size ± SD
M1	Cold uni-axial compacting step at 80 MPa + Temperature ramp of 5 °C/min up to 1300 °C under 17 MPa + Dwell for 1 h at 1300 °C under 80 MPa	90.0% ± 2.0 Geometrical method	340 ± 120 nm
M2	Cold uni-axial compacting step at 80 MPa + Temperature ramp of 5 °C/min up to 1975 °C at 17 MPa + Stage level for 1 h at 1975 °C and 80 MPa	97.3% ± 0.5 Archimedes' method	1.34 ± 0.66 μm
M3	Cold uni-axial compacting step at 80 MPa + Temperature ramp of 5 °C/min up to 1975 °C at 17 MPa + Stage level for 10 h at 1975 °C and 80 MPa	95.7% ± 0.5 Archimedes' method	24.80 ± 8.30 μm

We showed in previous work that the grain size obtained after sintering of TiN and TiC influences their behavior under irradiation and oxidation at high temperature [30–33]. Some other studies observed a potential gain in terms of resistance to irradiation of non-oxide ceramics due to submicron or nanometric grains [23,34]. This specific behavior of nanostructured ceramics is linked to the high density of grain boundaries (GBs) which favor the evacuation of some structural defects during irradiation [35]. These GBs are also expected to play a significant role in gas mobility and release in nuclear applications [36]. In fact, ceramic cladding must be a retention barrier to the fission products (FPs) during the fuel cycle as indicated previously. Among the FPs are inert gases which are mainly composed of Xe and Kr [35] (and He gas atoms from α-decay). These noble gases are known for their ability to form small clusters and gas bubbles at high concentrations. Bubble nucleation and growth can lead to substantial modification of the properties: decrease of thermal conductivity, crack propagation, creation of migration channels for other FPs. Although numerous noble-gas implantation studies have been performed on metals,

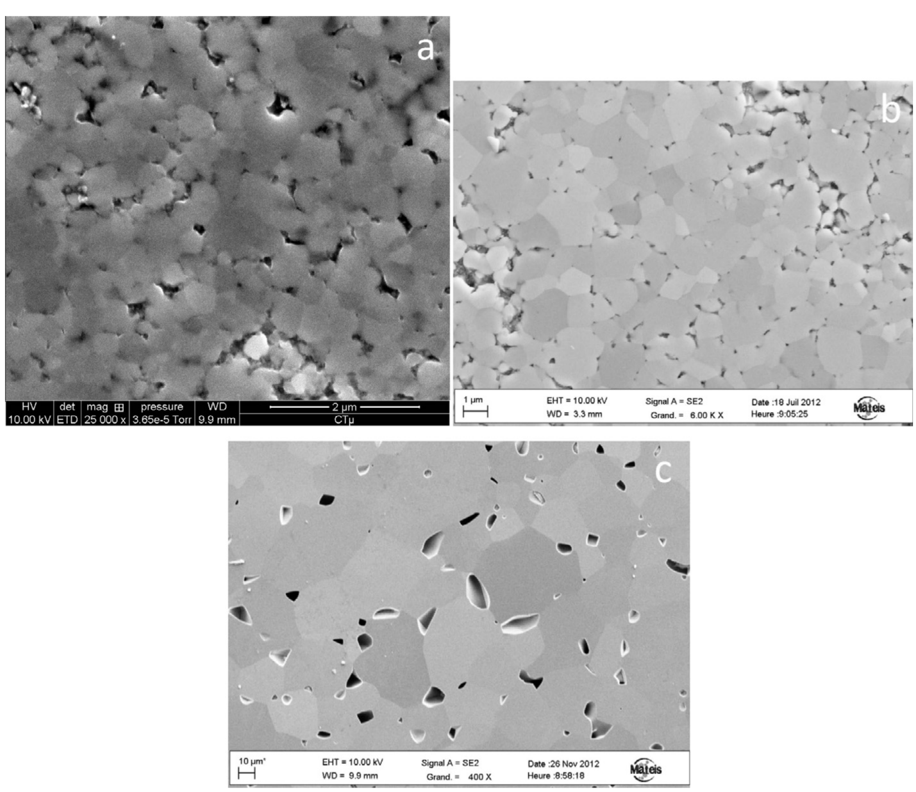

Fig. 1. SEM micrographs (secondary electrons) of the three initial microstructures: (a) M1, (b) M2 and (c) M3.